IEEE Access
Multidisciplinary | Rapid Review | Open Access Journal

SPECIAL SECTION ON INTELLIGENT LOGISTICS BASED ON BIG DATA

Received June 24, 2020, accepted July 10, 2020, date of publication July 20, 2020, date of current version July 30, 2020.

Digital Object Identifier 10.1109/ACCESS.2020.3010376

Modeling and Planning Multimodal Transport Paths for Risk and Energy Efficiency Using AND/OR Graphs and Discrete Ant Colony Optimization

ZHANZHONG WANG[1], MINGHANG ZHANG[1], RUIJUAN CHU[1], AND LIYING ZHAO[2]
[1]Transportation College, Jilin University, Changchun 130022, China
[2]School of Economics and Management, Xi'an University of Technology, Xi'an 710054, China

Corresponding author: Ruijuan Chu (1908950298@qq.com)

This work was supported in part by the National Natural Science Foundation of China under Grant 61873109 and in part by the Program of Humanities and Social Sciences, Ministry of Education under Grant 18YJA630157.

ABSTRACT Path sequence selection is important for multimodal transport processes. AND/OR graphs (AOG) have been applied to describe practical multimodal transport route planning problems by using 'AND' and 'OR' matrices. An AOG-based multimodal transport route planning problem is an NP-hard combinatorial optimization problem. Heuristic evolution methods can be adopted to handle it. While adjacency (AND) relationship issues can be addressed, contradiction (OR) relations are not well addressed by existing multimodal transport route planning methods. Thus, an ineffective result may be obtained in practice. The OR matrix is a conflict matrix that describes the choice of mode of transport in the process of multimodal transport. By using a contradiction matrix together with an adjacency matrix and tabu list, an approach used in existing work, this paper proposes an effective triple-phase generate route method (TPGR) to produce a feasible multimodal transport path sequence based on an AOG. This paper uses energy consumption to evaluate the multimodal transport energy efficiency. The information entropy is applied to describe the risks of the transport process. The energy consumption and the information entropy lead to a novel dual-objective optimization model where route energy consumption and route risk are minimized. An improved ant colony algorithm is developed to effectively generate a set of Pareto solutions for route selection, which are used for the dual-objective multimodal transport route optimization problem. This methodology is applied to practical multimodal transport route selection processes on two maps to verify its effectiveness and feasibility.

INDEX TERMS Multimodal transport, AND/OR graph, dual-objective discrete ant colony optimization, modeling and simulation.

I. INTRODUCTION

Due to a shortage of resources and environmental pollution, environmentally friendly transport has become vital to sustainable development and has attracted the attention of governmental regulators for a number of years. The risk of a path is also an important part of the multimodal transport process. Due to path risks, a large number of goods are damaged, delayed, or even unable to reach their destination each year. Therefore, it is important to choose appropriate paths in the transportation process.

Wang *et al.* [1] proposed a value-at-risk model based on an opportunity measure and determined the optimal route plan to minimize risks. Luan *et al.* [2] constructed a combined weighting model (consistency matrix analysis and information entropy method) to evaluate and prioritize the LRT network. Niven *et al.* [3] proposed a generalized maximum entropy framework to infer the state of a flowing network in the form of probability. Amari *et al.* [4] proposed a probability distribution manifold based on the entropy regularization of the optimal transport problem. Wang *et al.* [5] used the

The associate editor coordinating the review of this manuscript and approving it for publication was Di Wu.

information entropy method to determine the weight of each factor and the combined weight of each indicator in the urban traffic green evaluation index system. Liu *et al.* [6] compared the difference in traffic flow entropy of heavy trucks of different proportions. Chen *et al.* [7] transformed the solid transport model based on uncertain entropy into a deterministic equivalent model. Zhang *et al.* [8] proposed multivariate multi-scale distributed entropy (MMSDE). The complex entropy causality plane was used to evaluate the complexity of a traffic system. Zhang *et al.* [9] used the comprehensive evaluation method, combining information entropy theory and data envelopment analysis to evaluate the comprehensive benefits of enterprises. Dong *et al.* [10] adopted the traffic entropy model and the fuzzy c-mean method. The opening time was determined by calculating the entropy value and entropy generation of the boundary road network. Zhou *et al.* [11] introduced entropy to calculate the concealment degree of transportation, studied the concealment problem of military supply transportation in the whole network, and proposed the optimal flow distribution model. He *et al.* [12] studied the cluster of departure and destination (OD) trips and adopted entropy theory and probability distribution functions for parameter selection. Chai *et al.* [13] analyzed the complexity of dynamic network areasbased on the study of information entropy of natural structures in high dimensions in networks. Peng *et al.* [14] combined AHP and entropy- weighted methods, where the response taken by the stationwas used to obtain the risk rating of the risk factors.

Noussan *et al.* [15] proposed a scenario analysis for the future of European passenger transport by evaluating the potential effects of digitalization on mobility demand, energy consumption and CO_2 emissions under different assumptions. Wang *et al.* [16] presented a greenhouse gas emission and energy consumption accounting approach for on-road transportation. Fan *et al.* [17] introduced a new graphical decision-making tool to facilitate the rapid selection of transportation modes that minimize energy consumption or emissions, indicating the most sustainable transportation mode. Needell *et al.* [18] introduced a Trip Energy vehicle energy model capable of simulating the impact of traffic conditions on energy consumption and CO_2 emissions. Rehermann *et al.* [19] analyzed how GDP per capita affects transport energy consumption, testing possible nonlinear relationships between variables. Zhang *et al.* [20] presented an analysis of factors driving the market diffusion of EVs and the reasons for varying results across the investigated cities, in addition toestimates of related EV impacts on local energy consumption and CO_2 emissions.

Mnif *et al.* [21] introduced a new method for solving the problem of multimodal transport network planning to determine the optimal multimodal transport strategy. Laurent *et al.* [22] considered carbon emissions to construct multimodal transport planning decisions. Li *et al.* [23] established an intermediate route selection model for multimodal transport in a low-carbon environment. Sun *et al.* [24] modeled and optimized the freight routing problem in a road-railway multimodal transport network according to the network structure. Fan *et al.* [25] took the whole process of container multimodal transport as the research perspective to build a production system and analyze its operation process. Chen *et al.* [26] studied the route selection problem of multimodal transport to achieve the optimal balance between transportation time and transportation cost. Zhao *et al.* [27] constructed a multimodal transport cargo path system with vehicle availability and capacity constraints based on hierarchical co-simulation optimization (COSMO) methods.

To summarize, information entropy is widely used in transportation problems, and energy consumption is widely used in industrial problems. The research on multimodal transport is mainly focused on the optimization of transportation cost, while the research on the application of energy consumption and information entropy in multimodal transport is rare. Therefore, this paper constructs a multimodal transport paths optimization model with dual objectives that considers information entropy and energy consumption. Due to the characteristics of multimodal transport problems, a large number of infeasible solutions are generated in algorithm design. To handle it, we propose a triple-phase generate route method (TPGR) added to an improved ant colony algorithm that produces a large, diversified quantity of feasible solutions. Compared with existing research, we have two contributions: (1) To solve the adjacency (AND) and contradiction (OR) relations and constraints between paths of a multimodal transport AND/OR graph, we introduce adjacency and contradiction matrices. We also propose TPGR to produce feasible paths sequence solutions. (2) To solve a dual-objective multimodal transport path sequence optimization problem, we designed a dual-objective discrete ant colony algorithm (DDACO) producing Pareto solutions. It includes ant route representation, the evaluation of objective functions, pheromone updates, and multi-objective optimization.

II. PROBLEM STATEMENT

A. PROBLEM STATEMENT

This work handles the multimodal transport path plan problem from low risk and energy-efficient perspectives. Multimodal transport is a risky activity. Unforeseen situations such as bad weather and war may lead to longer transportation times, the loss of goods in transit, and the failure of goods to arrive at their intended destination. Thus, minimizing risk during the multimodal transport process is one optimization goal. Meanwhile, the multimodal transport process is an energy-intensive activity. Owing to growing energy usage and environmental concerns, energy consumption in a multimodal transport process is more and more important. Thus, minimizing energy consumption is another optimization goal. A multimodal program to minimize transport risk and energy consumption is subject to some specific constraints that we therefore propose to solve in this work.

The transportation of a particular batch of goods can usually take different routes, which is commonly expressed as sequences of paths selection. Paths selection sequencing involves graphically representing the set of all the possible path sequences and selecting the optimum sequence out of this set via heuristics, meta-heuristics, or mathematical programming. A path selection process for a given good can be represented by an AND/OR graph. Different multimodal transport paths, each of which is expressed via a feasible route sequence, are embodied in an undirected route AND/OR graph.

The undirected route AND/OR graph describes the adjacency and contradiction relations among paths. A variety of complex multimodal transport processes with multiple paths are frequent and typical in practice. In this work, the area affected by the risk is also taken into account. The basic ideas of AND/OR graphs are explained with a simulation multimodal transport map whose topological and geometric data, shown in the map drawing in Fig. 1, are converted to an AND/OR graph, shown in Fig. 2.

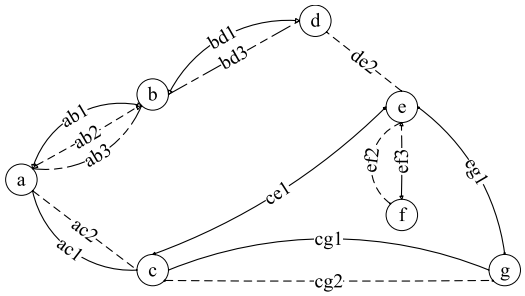

FIGURE 1. A simulation multimodal transport map.

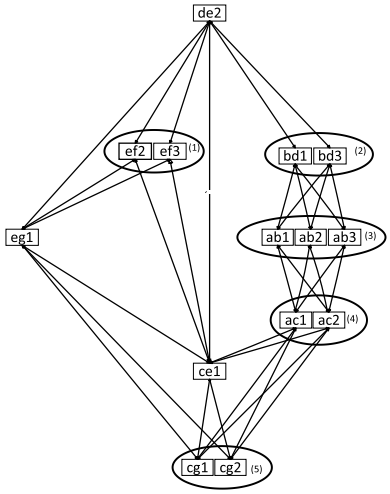

FIGURE 2. The AND/OR graph of the map in Fig. 1.

In Fig. 1, the nodes represent cities that can switch to different modes of transport. For example, at node a, the transport can be converted from road and rail to road, rail and water or from road, rail and water to road and rail. The path is expressed with an edge that is written by two nodes plus one number. The number means the mode of transport, specifically, that 1 is road transport, 2 is rail transport, and 3 is water transport. For example, the edge ab1 represents the path from node a to node b or from node b to node a with road transport. When two edges are connected by only one node, the paths represented by the two edges represent an adjacency relationship (AND relationship). When two edges are connected by two nodes, the paths represented by the two edges represent a contradiction relationship (OR relationship).

In Fig. 2, nodes represent a path that is the same as the edge in Fig. 1, and the edge represents an adjacency relationship (AND relationship). For example, after eg1 is selected, de2, ef2, ef3, ce1, cg1, and cg2 nodes can be selected. A hyper-edge represents a contradiction relationship (OR relationship). For example, the hyper-edge (3) has three nodes, ab1, ab2 and ab3. After ab1 is selected, ab2 and ab3 cannot be selected, which means that only one path can be selected between node a and node b in Fig. 1. The adjacency (and)/contradiction (or) relationship between paths can be represented by a matrix and obtained by calculation through incidence matrix F. The calculation method is shown in Fig. 3. There are four kinds of matrices in the Fig. 3, which are explained in the next part.

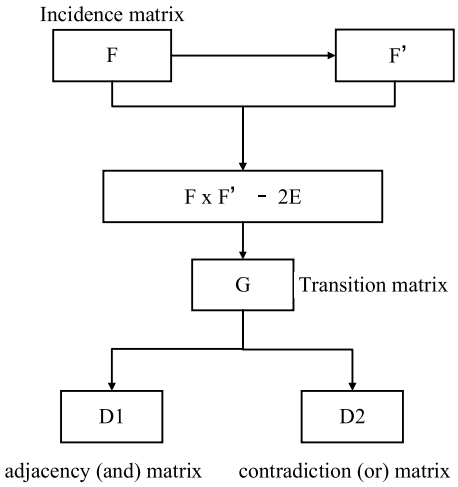

FIGURE 3. Adjacency (AND)/contradiction (OR) matrix generation flow chart.

The incidence matrix is the basis matrix in Fig. 3. It is a matrix whose rows correspond to paths and whose columns correspond to cities. If city is the endpoint of a path, the city is an incidence within the path. Each city is numbered by $1, 2, \ldots, I$ where I represents the number of cities. Each path is numbered by $1, 2, \ldots, J$ where J represents the number of paths. Note that this work adopts the incidence matrix $F = [f_{ij}]$ to represent the incidence relationship among cities and paths, and F' is the transpose of the matrix F

$$f_{ij} = \begin{cases} 1 & \textit{if city } i \textit{ is an incidence in path } j \\ 0 & \textit{otherwise} \end{cases}$$

Thus, the incidence matrix F of the map shown in Fig. 3 is expressed as:

$$F = \begin{array}{c} ab1 \\ ab2 \\ ab3 \\ ac1 \\ ac2 \\ bd1 \\ bd3 \\ ce1 \\ cg1 \\ cg2 \\ de2 \\ ef2 \\ ef3 \\ eg1 \end{array} \begin{bmatrix} 1 & 1 & 0 & 0 & 0 & 0 & 0 \\ 1 & 1 & 0 & 0 & 0 & 0 & 0 \\ 1 & 1 & 0 & 0 & 0 & 0 & 0 \\ 1 & 0 & 1 & 0 & 0 & 0 & 0 \\ 1 & 0 & 1 & 0 & 0 & 0 & 0 \\ 0 & 1 & 0 & 1 & 0 & 0 & 0 \\ 0 & 1 & 0 & 1 & 0 & 0 & 0 \\ 0 & 0 & 1 & 0 & 1 & 0 & 0 \\ 0 & 0 & 1 & 0 & 0 & 0 & 1 \\ 0 & 0 & 1 & 0 & 0 & 0 & 1 \\ 0 & 0 & 0 & 1 & 1 & 0 & 0 \\ 0 & 0 & 0 & 0 & 1 & 1 & 0 \\ 0 & 0 & 0 & 0 & 1 & 1 & 0 \\ 0 & 0 & 0 & 0 & 1 & 0 & 1 \end{bmatrix}$$

The transition matrix G is calculated by:

$$G = F * F' - 2 * E$$

E is the identity matrix. G has two properties that can be used in the next part and section III.

Define a set $V = \{n, d\}$ where n represents a point (city) in incidence matrix F. Let d represent an edge (path) in incidence matrix F such that $d = \{n_1, n_2\}$, where n_1 and n_2 are the endpoints of d.

Property 1: the transition matrix G only contains 0, 1 and 2 elements.

Proof: define $d_j = \{n_{j1}, n_{j2}\}$, $d_k = \{n_{k1}, n_{k2}\}$, where j, k represent any edge serial number. When $j \neq k$, $n_{j1} = n_{k1}$ & $n_{j2} \neq n_{k2}$, we obtain $d_j \cap d_k = \{n_{j1}\}$, $||d_j \cap d_k|| = 1$. When $j \neq k$, $n_{j1} = n_{k1}$ & $n_{j2} = n_{k2}$, we obtain $d_j \cap d_k = \{n_{j1}, n_{j2}\}$, $||d_j \cap d_k|| = 2$. When $j \neq k$, $n_{j1} \neq n_{k1}$ & $n_{j2} \neq n_{k2}$, we obtain $d_j \cap d_k = \{\Phi\}$, $||d_j \cap d_k|| = 0$. The numerical of the matrix G represents the norm value of the intersection of the vertices of two edges, indicating that there are only norm values 0, 1, 2 in the transition matrix G.

Property 2: the value of the elements on the main diagonal of the matrix obtained by the transition matrix G is 0

Proof: define $d_j = \{n_{j1}, n_{j2}\}$, $d_k = \{n_{k1}, n_{k2}\}$, When $j = k$, we obtain $d_j \cap d_k = \{n_{j1}, n_{j2}\}$, $||d_j \cap d_k|| = 2$. Since the diagonal operation conforms to $i = j$, the element values on it are all 2.

This work adopts transition matrix $G = [g_{jk}]$ to represent the relationship among paths. j, k denotes any path in G. According to Property 1, we obtain

$$g_{jk} = \begin{cases} 2 & \textit{if } j \textit{ is contradiction relationship with } k \\ 1 & \textit{if } j \textit{ is adjacency relationship with } k \\ 0 & \textit{otherwise} \end{cases}$$

Thus, the transition matrix G of the map shown in Fig. 2 is expressed as:

$$G = \begin{bmatrix} 0 & 2 & 2 & 1 & 1 & 1 & 1 & 0 & 0 & 0 & 0 & 0 & 0 & 0 \\ 2 & 0 & 2 & 1 & 1 & 1 & 1 & 0 & 0 & 0 & 0 & 0 & 0 & 0 \\ 2 & 2 & 0 & 1 & 1 & 1 & 1 & 0 & 0 & 0 & 0 & 0 & 0 & 0 \\ 1 & 1 & 1 & 0 & 2 & 0 & 0 & 1 & 1 & 1 & 0 & 0 & 0 & 0 \\ 1 & 1 & 1 & 2 & 0 & 0 & 0 & 1 & 1 & 1 & 0 & 0 & 0 & 0 \\ 1 & 1 & 1 & 0 & 0 & 0 & 2 & 0 & 0 & 0 & 1 & 0 & 0 & 0 \\ 1 & 1 & 1 & 0 & 0 & 2 & 0 & 0 & 0 & 0 & 1 & 0 & 0 & 0 \\ 0 & 0 & 0 & 1 & 1 & 0 & 0 & 0 & 1 & 1 & 1 & 1 & 1 & 1 \\ 0 & 0 & 0 & 1 & 1 & 0 & 0 & 1 & 0 & 2 & 0 & 0 & 0 & 1 \\ 0 & 0 & 0 & 1 & 1 & 0 & 0 & 1 & 2 & 0 & 0 & 0 & 0 & 1 \\ 0 & 0 & 0 & 0 & 0 & 1 & 1 & 1 & 0 & 0 & 0 & 1 & 1 & 1 \\ 0 & 0 & 0 & 0 & 0 & 0 & 0 & 1 & 0 & 0 & 1 & 0 & 2 & 1 \\ 0 & 0 & 0 & 0 & 0 & 0 & 0 & 1 & 0 & 0 & 1 & 2 & 0 & 1 \\ 0 & 0 & 0 & 0 & 0 & 0 & 0 & 1 & 1 & 1 & 1 & 1 & 1 & 0 \end{bmatrix}$$

According to transition matrix G, adjacency matrix D_1 and contradiction matrix D_2 are obtained separately. This work adopts adjacency matrix $D_1 = [d_{1jk}]$ to represent the adjacency relationship among paths, where path j, k means any path in D_1. Since the element with number 1 in the transition matrix G represents an adjacency relation, this part is extracted as adjacency matrix D_1.

$$d_{1jk} = \begin{cases} 1 & \textit{if path } j \textit{ is adjacency with path } k \\ 0 & \textit{otherwise} \end{cases}$$

Thus, the adjacency matrix D_1 of the map shown in Fig. 2 is expressed as:

$$D_1 = \begin{bmatrix} 0 & 0 & 0 & 1 & 1 & 1 & 1 & 0 & 0 & 0 & 0 & 0 & 0 & 0 \\ 0 & 0 & 0 & 1 & 1 & 1 & 1 & 0 & 0 & 0 & 0 & 0 & 0 & 0 \\ 0 & 0 & 0 & 1 & 1 & 1 & 1 & 0 & 0 & 0 & 0 & 0 & 0 & 0 \\ 1 & 1 & 1 & 0 & 0 & 0 & 0 & 1 & 1 & 1 & 0 & 0 & 0 & 0 \\ 1 & 1 & 1 & 0 & 0 & 0 & 0 & 1 & 1 & 1 & 0 & 0 & 0 & 0 \\ 1 & 1 & 1 & 0 & 0 & 0 & 0 & 0 & 0 & 0 & 1 & 0 & 0 & 0 \\ 1 & 1 & 1 & 0 & 0 & 0 & 0 & 0 & 0 & 0 & 1 & 0 & 0 & 0 \\ 0 & 0 & 0 & 1 & 1 & 0 & 0 & 0 & 1 & 1 & 1 & 1 & 1 & 1 \\ 0 & 0 & 0 & 1 & 1 & 0 & 0 & 1 & 0 & 0 & 0 & 0 & 0 & 1 \\ 0 & 0 & 0 & 1 & 1 & 0 & 0 & 1 & 0 & 0 & 0 & 0 & 0 & 1 \\ 0 & 0 & 0 & 0 & 0 & 1 & 1 & 1 & 0 & 0 & 0 & 1 & 1 & 1 \\ 0 & 0 & 0 & 0 & 0 & 0 & 0 & 1 & 0 & 0 & 1 & 0 & 0 & 1 \\ 0 & 0 & 0 & 0 & 0 & 0 & 0 & 1 & 0 & 0 & 1 & 0 & 0 & 1 \\ 0 & 0 & 0 & 0 & 0 & 0 & 0 & 1 & 1 & 1 & 1 & 1 & 1 & 0 \end{bmatrix}$$

This work adopts contradiction matrix $D_2 = [d_{2jk}]$ to represent the contradiction relationship among paths, where path j, k means any path in D_2. Since the element with number 2 in the transition matrix G represents a contradiction relation, this part is extracted as the contradiction matrix D_2.

$$d_{2jk} = \begin{cases} 2 & \textit{if path } j \textit{ is contradiction with path } k \\ 0 & \textit{otherwise} \end{cases}$$

Thus, contradiction matrix D_2 of the map shown in Fig. 2 is expressed as:

$$D_2 = \begin{bmatrix} 0 & 2 & 2 & 0 & 0 & 0 & 0 & 0 & 0 & 0 & 0 & 0 & 0 \\ 2 & 0 & 2 & 0 & 0 & 0 & 0 & 0 & 0 & 0 & 0 & 0 & 0 \\ 2 & 2 & 0 & 0 & 0 & 0 & 0 & 0 & 0 & 0 & 0 & 0 & 0 \\ 0 & 0 & 0 & 0 & 2 & 0 & 0 & 0 & 0 & 0 & 0 & 0 & 0 \\ 0 & 0 & 0 & 2 & 0 & 0 & 0 & 0 & 0 & 0 & 0 & 0 & 0 \\ 0 & 0 & 0 & 0 & 0 & 0 & 2 & 0 & 0 & 0 & 0 & 0 & 0 \\ 0 & 0 & 0 & 0 & 0 & 2 & 0 & 0 & 0 & 0 & 0 & 0 & 0 \\ 0 & 0 & 0 & 0 & 0 & 0 & 0 & 0 & 0 & 0 & 0 & 0 & 0 \\ 0 & 0 & 0 & 0 & 0 & 0 & 0 & 0 & 0 & 2 & 0 & 0 & 0 \\ 0 & 0 & 0 & 0 & 0 & 0 & 0 & 0 & 2 & 0 & 0 & 0 & 0 \\ 0 & 0 & 0 & 0 & 0 & 0 & 0 & 0 & 0 & 0 & 0 & 0 & 0 \\ 0 & 0 & 0 & 0 & 0 & 0 & 0 & 0 & 0 & 0 & 0 & 2 & 0 \\ 0 & 0 & 0 & 0 & 0 & 0 & 0 & 0 & 0 & 0 & 2 & 0 & 0 \\ 0 & 0 & 0 & 0 & 0 & 0 & 0 & 0 & 0 & 0 & 0 & 0 & 0 \end{bmatrix}$$

Each path needs to consume some energy during transport. A feasible route path should satisfy a specific length constraint to reduce energy consumption for a route selection process.

In addition, as shown in Fig. 2, to reach different multimodal transport routes, different paths to solutions may be generated. This work aims to determine and select Pareto solutions among the paths to minimize multimodal transport risk while also minimizing the total multimodal transport energy consumption to meet the specific energy consumption requirement. We call this problem the multimodal transport route sequence optimization problem based on an AND/OR graph from risk and energy-efficiency perspectives.

B. MATHEMATICAL MODEL

1) i,j— the index of a multimodal transport path, with $i, j \in \{1, 2, 3, \ldots, N\}$, where N is the number of all multimodal transport paths in a given AND/OR graph

2) c_i—the per weight energy consumed per unit transport length of path i

3) C_{ij}—the per weight energy consumed of conversion from multimodal transport path i to multimodal transport path j

4) L_i— the length of multimodal transport path i

5) P_i— the probability of the risk of multimodal transport path i

6) Q_i— the maximum capacity of multimodal transport path i

7) q— the goods' weight

8) D_1— adjacency matrix(AND matrix) of multimodal transport path

9) D_2— contradiction matrix(OR matrix) of multimodal transport path

10) Qs— full permutation matrix, which represents whether there are risk situations in the selected multimodal transport. Qs is 0 in the case of a risk situation or 1 in the case of a risk situation

Decision variables:

$x_i : x_j = 1$ if multimodal transport path i is performed, otherwise, $x_i = 0$.

By considering the two goals of minimizing multimodal transport route information entropy and minimizing multimodal transport route energy consumption, a dual-objective multimodal transport path sequence plan problem model subject to multiple constraints is given as follows:

$$\min f_1 = C_{path} + C_{transformation} \tag{1}$$

The objective of function f_1 is to minimize energy consumption when selecting the multimodal transport route, where its first item in (1) is obtained energy consumption during transportation, and where its second item in (1) is obtained energy consumption during transformation transportation mode.

$$C_{path} = \sum_{i=1}^{N} x_i * L_i * c_i * q \tag{2}$$

The energy consumption during transportation is expressed in (2), which represents the energy consumption of goods in transit. Where, L_i is the length of multimodal transport path i. c_i is the per weight energy consumed per unit transport length of path i.

$$C_{transformation} = \sum_{j=1}^{N} \sum_{i=1}^{N} \lfloor (D_{1ij} + x_i * x_j)/2 \rfloor * C_{ij} * q \tag{3}$$

The energy consumption during transformation transportation mode is expressed in (3), which represents energy consumption when goods are changing transportation mode. Where, D_{1ij} is the element of the adjacency matrix. C_{ij} is the per weight energy consumed of conversion. q is the goods' weight.

$$\min f_2 = \sum_{b=1}^{2^{sx}} I_b \tag{4}$$

The objective of function f_2 is to minimize information entropy, which represents the route risk in (4). Where, I_b is the amount of information. The time complexity of information entropy calculation can be obtained as $O(2^{sx})$, sx is the length of the selected path.

$$sx = \sum_{i=1}^{N} x_i \tag{5}$$

sx represents the number of the paths that are selected in (5).

$$I_b = -1 * Ps_b * \log_2 Ps_b \quad b = 1, 2, \ldots, sx \tag{6}$$

I_b represents the amount of information from which some path risks occur in (6). $b = 1, 2, \ldots, sx$, where sx is the number of path risk combinations.

$$Ps_b = \prod_{i=1}^{N} |Qs_{bi} - P_i * x_i| \quad b = 1, 2, \ldots, sx \tag{7}$$

Ps_b represents probability at which some path risks occur in (7). Where, Qs is a matrix, which represents all of the cases in the risk. The elements of sx are only 0 and 1 in the paths obtained and is otherwise 0. For example, when $sx = 3$, paths 4, 8, 12 are obtained. Qs can be obtained:

$$Qs = \begin{bmatrix} 0 & 0 & 0 & 0 & 0 & 0 & 0 & 0 & 0 & 0 & 0 & 0 & 0 \\ 0 & 0 & 0 & 0 & 0 & 0 & 0 & 0 & 0 & 0 & 1 & 0 & 0 \\ 0 & 0 & 0 & 0 & 0 & 0 & 0 & 1 & 0 & 0 & 0 & 0 & 0 \\ 0 & 0 & 0 & 0 & 0 & 0 & 0 & 1 & 0 & 0 & 0 & 1 & 0 \\ 0 & 0 & 0 & 1 & 0 & 0 & 0 & 0 & 0 & 0 & 0 & 0 & 0 \\ 0 & 0 & 0 & 1 & 0 & 0 & 0 & 0 & 0 & 0 & 0 & 1 & 0 \\ 0 & 0 & 0 & 1 & 0 & 0 & 0 & 1 & 0 & 0 & 0 & 0 & 0 \\ 0 & 0 & 0 & 1 & 0 & 0 & 0 & 1 & 0 & 0 & 0 & 1 & 0 \end{bmatrix}$$

$$Q_i - q * x_i \geq 0 \quad i = \{1, 2, \ldots, N\} \tag{8}$$

Constraint (8) ensures that the goods' weight is no more than the max capacity in path i. Where, Q_i is the maximum capacity of multimodal transport path i. q is the goods' weight.

$$\begin{cases} \sum_{\substack{j=1 \\ j \neq O}}^{N} \lfloor (D_{1ij} + x_i * x_j)/2 \rfloor = 1 & i = O \\ \sum_{\substack{j=1 \\ j \neq i}}^{N} \lfloor (D_{1ij} + x_i * x_j)/2 \rfloor = 2 & i \neq O, i \neq D \\ \sum_{\substack{j=1 \\ j \neq D}}^{N} \lfloor (D_{1ij} + x_i * x_j)/2 \rfloor = 1 & i = D \end{cases} \tag{9}$$

Constraint (9) represents a multimodal transport route sequence that must be continuous from starting point to end point. There is only one edge adjacent to the starting edge and the ending edge. There are two edges adjacent to the other edges. Where, D_{1ij} is the element of adjacency matrix. O is the starting path, and D is the ending path. i is that path that has been selected.

$$\sum_{i=1}^{N} x_i \leq \sum_{i=1}^{N} (1/(\sum_{j=1}^{N} D_{2ij}/2 + 1)) \tag{10}$$

Constraint (10) represents the number of selected paths that must be less than are stricted quantity. Where, D_{2ij} is the element of contradiction matrix.

$$\sum_{j=1}^{N} (x_j * D_{2ij}/2) = 0 \tag{11}$$

Constraint (11) ensures that there can be only one mode of transportation between two adjacent multimodal transport nodes, where, $D_{2ij}/2 = 1$ represent or relationship between i and j.

$$0 \leq P_i * x_i \leq 0.5 \tag{12}$$

Constraint (12) represents the max probability of multimodal transport path risk, which must be less than 0.5. When the maximum probability of multimodal transport path risk is greater than 0.5, the ability of the model to find the multimodal transport route with less risk is affected by the information entropy formula. In addition, the min probability of multimodal transport path risk must be greater than 0. Where, P_i is the probability of the risk.

III. THE PROPOSED ALGORITHM

This work proposes an evolutionary heuristic algorithm which can quickly solve large-scale industrial problems [28]–[33] called DDACO. The method can be applied to an expandable AND/OR graph. This enables the gradual increase of map complexity to handle large-scale complex route optimization problem due to strong search ability of evolutionary heuristic algorithm. It is demonstrated that the convergence of the evolution process is satisfactory, and the required CPU time appears comparatively small and only moderately increases with the number of constraints. The method can be applied to questions with a complexity that cannot be managed with an exact method.

There are few control parameters and well optimization effects in the ACO algorithm [34]–[39], which are its main advantages. Due to its simplicity and ease of implementation, it has gained more and more attention and has been used to solve many practical and complex industrial optimization problems [40]–[45]. Hence, we used ACO to solve our proposed multimodal transport route sequence optimization problem.

However, the basic ACO algorithm was originally designed for continuous function optimization instead of our proposed integer programming model. In addition, the two objectives of the proposed model form Pareto solutions, which are different from the single objective problem in the basic ACO algorithm. Thus, in order to make it applicable for solving the problem considered, we established a novel dual-objective discrete version of the ACO algorithm, named DDACO. As is known, a non-dominated sorting approach in NSGA-II [46]–[50] is one of the most popular and widely used algorithms to solve multi-objective optimization problems due to its excellent performance. Hence, this work adopted a non-dominated sorting procedure to produce a set of Pareto solutions and update an external Pareto solutions archive.

The proposed solution approach consists of four phases: A) ant route representation, B) evaluation of objective functions, C) pheromone update, D) multi-objective optimizer, and E) termination rules.

A. ANT ROUTE REPRESENTATION

The ant route represents a solution vector of a multimodal transport path sequence. As the basic characteristic of our problem, a single-link list method is selected as an encoding one. Namely, an ant route is expressed by $S = \{L_1, \ldots, L_k, \ldots, L_n\}$ where s_k is encoded by binary number (0 or 1) and n is the number of paths. For example,

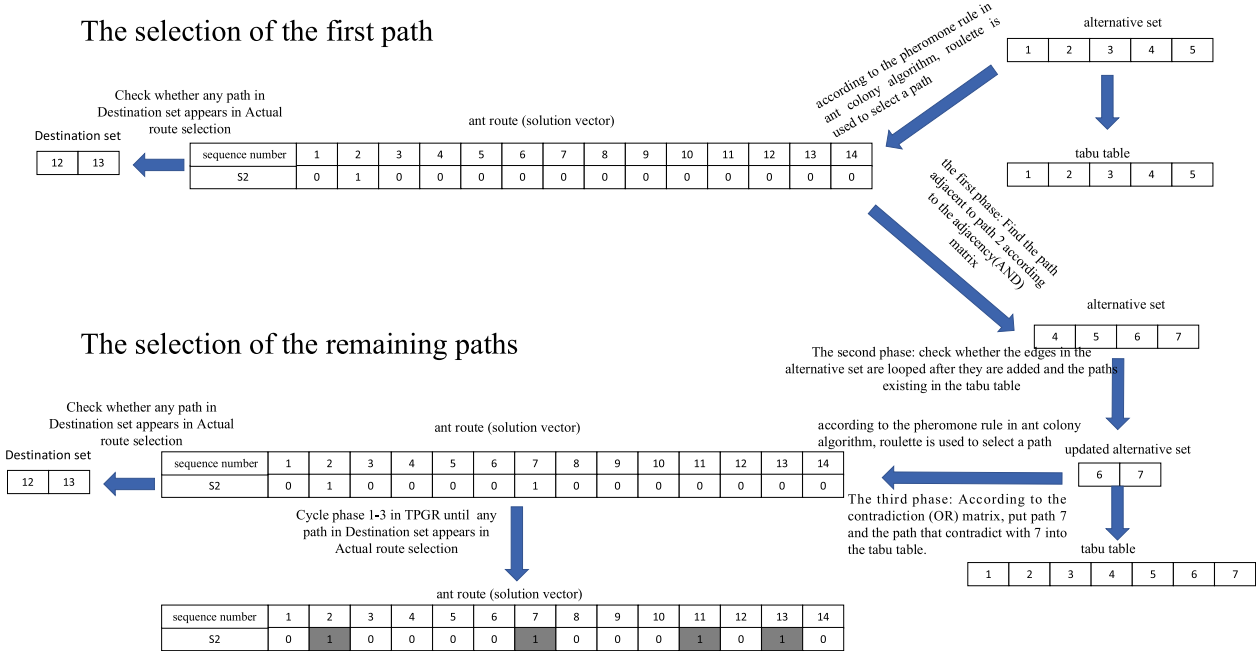

FIGURE 4. Triple-phase generate route.

$S = \{0, 1, 0, 0, 0, 0, 1, 0, 0, 0, 1, 0, 1, 0\}$ denotes that path 2, path 7, path 11 and path13in S are performed.

As is known, the first problem to be solved in a multimodal transport route sequence optimization problem is the rapid creation of feasible multimodal transport route solutions since multiple potential constraint requirements, listed in Section II, exist. Particularly, solving a multimodal transport path sequence problem should produce a great number of feasible solutions for the quasi-optimal or optimal solutions in the whole iterative evolution. Thus, we propose a triple-phase generate route (TPGR) excepting the first path generated, which satisfies the potential constraint requirement.

TPGR includes three phases. The first phase is to choose the adjacent paths. The second phase is to screen out adjacent paths that are not feasible for meeting constraints 10 and 11. The third phase is to put the appropriate path into a solution vector and update the tabu table. Due to the use of TPGR, constraints 9-11 are satisfied. The proposed ant route with TPGR carries out the following steps:

The selection of the first path: To do so, we first introduce an alternative set, which includes alternate paths and a tabu table, including selected paths and paths that are contradictory with selected paths. We then put the paths adjacent to the starting point into the alternate set. According to the pheromone rule in the ant colony algorithm, roulette is used to select a path A in the alternative set and put it into the ant route (solution vector). Then, we put the paths in the alternative set into the tabu table. If any path in the ant route (solution vector) is adjacent to the termination point, the path generation process ends, otherwise the path generation process continues.

For example, in Fig. 1, we first put the paths {1(a-b[1]), 2(a-b[2]), 3(a-b[3]), 4(a-c[1]), 5(a-c[2])} into the alternate set, which is adjacent to the starting point a. Second, we choose path 2 to place into the ant route (solution vector). Finally, we put the paths {1(a-b[1]), 2(a-b[2]), 3(a-b[3]), 4(a-c[1]), 5(a-c[2])} into the tabu table, as shown in Fig. 4.

The selection of the remaining paths: first, according to the path adjacency (AND) matrix, all paths adjacent to the last path of the ant route (solution vector) are put into the alternative set. Second, we should check whether the paths in the alternative set are looped in the AND/OR graph after they are added into the ant route (solution vector), and, if so, remove them from the alternative set. The paths in the tabu table are also removed. According to the pheromone rules in the ant colony algorithm, roulette is used to select a path B in the alternative set and put it into the ant route (solution vector). Third, according to the contradiction (OR) matrix, we put path B and the paths that contradict B into the tabu table. Finally, if a path in the ant route (solution vector) is adjacent to the termination point, the path generation process ends; otherwise, the path generation process continues.

For example, in Fig. 1, we first see that according to the path adjacency (AND) matrix, {4(a-c[1]), 5(a-c[2]), 6(b-d[1]), 7(b-d[3])} should be put into the alternative set. In the second phase, we remove {4(a-c[1]), 5(a-c[2])} from the alternative set that exists in the tabu table. The path 7(b-d[3]) is placed into the ant route(solution vector). In the third phase, according to the contradiction (OR) matrix, we put path 7 and path 6, which contradicts with path 7, into the tabu table, as shown in Fig. 4.

TABLE 1. The path corresponds to the mode of multimodal transportation.

path	a b[1]	a-b[2]	a -b[3]	a-c[1]	a-c[2]	b-d[1]	b-d[3]	c-e[1]	c-g[1]	c-g[2]	d-e[2]	e-f[2]	e-f[3]	e-g[1]
Mode	road	rail	water	road	rail	road	water	road	road	rail	rail	rail	water	road

TABLE 2. Length of path in multimodal transportation.

path	a-b[1]	a-b[2]	a-b[3]	a-c[1]	a-c[2]	b-d[1]	b-d[3]	c-e[1]	c-g[1]	c-g[2]	d-e[2]	e-f[2]	e-f[3]	-g[1]
distance	3213	3152	2815	3241	3132	3332	2154	1232	1321	1113	1221	523	311	299

TABLE 3. The transport resource capacity of path in multimodal transportation.

path	a-b[1]	a-b[2]	a-b[3]	a-c[1]	a-c[2]	b-d[1]	b-d[3]	c-e[1]	c-g[1]	c-g[2]	d-e[2]	e-f[2]	e-f[3]	e-g[1]
capacity	10	3	5	10	3	10	5	10	10	3	3	3	5	10

From Fig. 4, we can clearly see that the generated multimodal transport route solution/sequence is 2(a-b[2])→7(b-d[3])→11(d-e[2])→13(e-f[3])(shaded). Due to the characteristics of a multimodal transport route optimization problem, it is rather hard to obtain a feasible solution for a heuristic algorithm with the abovementioned generation. Generally, as the number of operations grows, the number of solutions increases rapidly, which implies that the probability of producing an infeasible solution can be great, especially for some large-scale multimodal transport route optimization processes. Thus, TPGR is significant in order for this problem to be solved.

B. EVALUATION OF OBJECTIVE FUNCTIONS

It is necessary to evaluate an ant route solution. It is composed of two objectives: energy consumption and information entropy. The evaluation of the ant route solution, which represents a multimodal route, is calculated by the objective function. For example, the energy consumption of the route a-c[2]→c-g[2]→e-g[1]→e-f[2] is 2614.25J,and the information entropy of the route a-c[2]→c-g[2]→e-g[1]→e-f[2] is 1.1114bit.

C. PHEROMONE UPDATE

The two fitness values of each ant are calculated. According to the results of the dual-objective optimizer, the non-dominant solution set in the current iteration times was recorded, and the pheromone concentration on the connecting path of each city was updated according to formula (13) and formula (14). In addition, we updated the probability that each path is selected, according to the pheromone update result in formula (15).

$$\begin{cases} \tau_{ij}(t+1) = (1-\rho) * \tau_{ij}(t) + \Delta\tau_{ij} \\ \Delta\tau_{ij} = \sum_{k=1}^{m} \Delta\tau_{ij}^{k} \end{cases} \quad i, j = 1, 2, \ldots, N \quad (13)$$

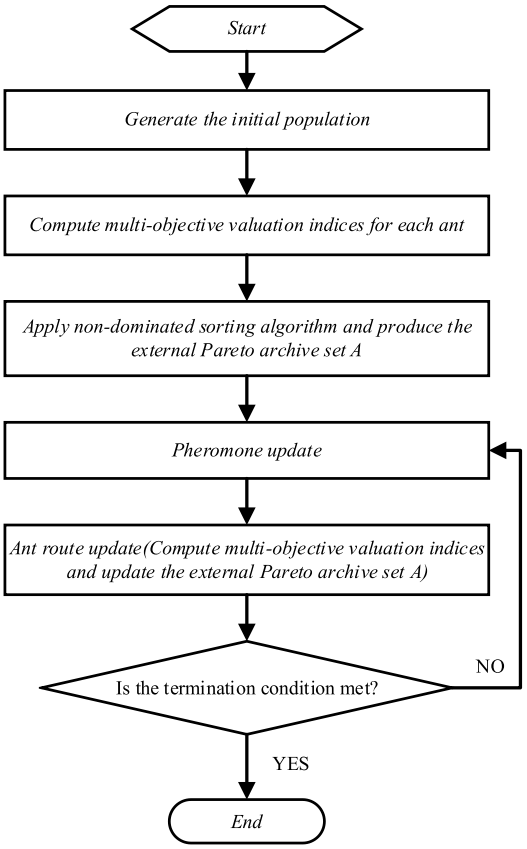

FIGURE 5. The outline of DDACO algorithm.

$\Delta\tau_{ij}^{k}$ represents the pheromone concentration released by the kth ant on the connection path between node i and node j, where m is the number of ants. τ_{ij} represents the sum of the pheromone concentrations released by all ants on the connection path between node i and node j, and t represents iteration in formula (13).

$$\Delta\tau_{ij}^{k} = \begin{cases} Q & \text{The kth ant accesses path i from path j} \\ 0 & \text{otherwise} \end{cases} \quad (14)$$

TABLE 4. Energy consumption in switching modes of transport.

Energy consumption	Road transportation	Railway transportation	Waterway transport
Road transportation	0	3	2
Railway transportation	3	0	4
Waterway transport	2	4	0

TABLE 5. Starting point and ending point.

Begin point	The path associated with the starting point	End point	The path associated with the starting point
a	a-b[1], a-b[2], a-b[3], a-c[1], a-c[2]	g	e-f[2], e-f[3]

TABLE 6. The probability of risk in multimodal transportation.

path	a-b[1]	a-b[2]	a-b[3]	a-c[1]	a-c[2]	b-d[1]	b-d[3]	c-e[1]	c-g[1]	c-g[2]	d-e[2]	e-f [2]	e-f [3]	e-g[1]
Probability%	13	2	8	2	30	5	12	3	11	2	4	11	3	1

TABLE 7. The speed of transport mode in multimodal transportation.

	Road transportation	Railway transportation	Waterway transport
Speed of transport	4	2	1

TABLE 8. Energy consumption per unit time of different modes of transportation.

	Road transportation	Railway transportation	Waterway transport
Energy consumption	3	1	0.5

TABLE 9. Produced Pareto solutions for case study 1.

runs	No.	Set of routes	f1(J)	f2(bit)	Used time（s）
1	1	a-c[2]→c-g[2]→e-g[1]→e-f[2]	2614.25	1.1114	9.5657
	2	a-c[1]→c-g[2]→e-g[1]→e-f[3]	3375	0.8629	
	3	a-c[1]→c-e[1]→e-f[2]	3619.25	0.5793	
	4	a-c[2]→c-g[2]→e-g[1]→e-f[3]	2507.25	1.3758	
	5	a-c[1]→c-g[2]→e-g[1]→e-f[2]	3482	0.5986	
	6	a-c[2]→c-e[1]→e-f[2]	2757.50	1.0921	
2	1	a-c[1]→c-g[2]→e-g[1]→e-f[2]	3482	0.5986	10.4116
	2	a-c[1]→c-e[1]→e-f[2]	3619.25	0.5793	
	3	a-c[1]→c-g[2]→e-g[1]→e-f[3]	3375	0.8629	
	4	a-c[2]→c-g[2]→e-g[1]→e-f[3]	2507.25	1.3758	
	5	a-c[2]→c-e[1]→e-f[2]	2757.50	1.0921	
	6	a-c[2]→c-g[2]→e-g[1]→e-f[2]	2614.25	1.1114	
3	1	a-c[1]→c-g[2]→e-g[1]→e-f[3]	3375	0.8629	10.3682
	2	a-c[1]→c-e[1]→e-f[2]	3619.25	0.5793	
	3	a-c[2]→c-g[2]→e-g[1]→e-f[2]	2614.25	1.1114	
	4	a-c[1]→c-g[2]→e-g[1]→e-f[2]	3482	0.5986	
	5	a-c[2]→c-e[1]→e-f[2]	2757.50	1.0921	
	6	a-c[2]→c-g[2]→e-g[1]→e-f[3]	2507.25	1.3758	

$\Delta\tau_{ij}^{k}$ means that the pheromone released each time is a constant value in formula (14)

$$P_{ij}^{k}(t)=\tau_{ij}(t)/\sum_{j=1}^{N}\tau_{ij}(t)\quad k=1,2,\ldots,m\quad i,j=1,2,\ldots,N \tag{15}$$

P_{ij}^{k} represents the probability of the t iteration ant k transferring from node i to node j, and N represents the number of nodes in formula (15).

D. MULTI-OBJECTIVE OPTIMIZER

This work solves the retention rules of the algorithm iterations and uses a non-dominated sort algorithm to divide

TABLE 10. Produced Pareto solutions for case study 2.

runs	No.	Set of routes	f1(J)	f2(bit)	Used time（s）
1	1	K-W[1]→W-AG[2]	1253	1.0335	256.7778
	2	K-W[1]→W-AG[1]	1500	0.8454	
	3	K-W[1]→W-AG[2]	1000	1.2217	
	4	K-L[2]→L-M[2]→M-N[2]→N-O[2]→O-AD[2]→AD-AG[1]	4728	0.3115	
	5	K-L[2]→L-M[1]→M-N[1]→N-O[1]→O-AD[2]→AD-AG[2]	5406	0.2624	
	6	K-L[1]→(L-M[2]→W-M[1]→W-AG[1]	3381	0.7765	
	7	K-L[1]→L-M[1]→M-N[2]→N-O[1]→O-AD[1]→AD-AG[1]	6156	0.2134	
	8	K-L[1]→L-M[1]→M-N[2]→N-O[1]→O-AD[1]→AD-AG[2]	5784	0.2379	
	9	K-L[1]→L-M[1]→M-N[1]→N-O[1]→O-AD[1]→AD-AG[1]	6525	0.1889	
2	1	K-W[2]→W-AG[2]	1000	1.2217	264.8723
	2	K-W[1]→W-AG[1]	1500	0.8454	
	3	K-W[2]→W-AG[1]	1253	1.0336	
	4	K-L[2]→L-M[2]→W-M[1]→W-AG[1]	3003	0.8011	
	5	K-L[2]→L-M[1]→M-N[2]→N-O[2]→O-AD[2]→AD-AG[2]	4656	0.3115	
	6	K-L[2]→L-M[1]→W-M[1]→W-AG[1]	3303	0.7766	
	7	K-L[2]→L-M[1]→M-N[2]→N-O[2]→O-AD[1]→AD-AG[1]	5409	0.2624	
	8	K-L[2]→L-M[1]→M-N[1]→N-O[1]→O-AD[2]→AD-AG[1]	5784	0.2379	
	9	K-L[1]→L-M[2]→M-N[1]→N-O[1]→O-AD[2]→AD-AG[2]	5484	0.2624	
3	1	K-L[2]→L-M[1]→M-N[2]→N-O[2]→O-AD[2]→AD-AG[2]	4656	0.3115	331.3379
	2	K-W[2]→W-AG[1]	1253	1.0336	
	3	K-W[2]→W-AG[2]	1000	1.2217	
	4	K-L[2]→L-M[2]→M-N[2]→N-O[1]→O-AD[1]→AD-AG[1]	5478	0.2624	
	5	K-W[1]→W-AG[1]	1500	0.8454	
	6	K-L[1]→L-M[1]→M-N[1]→N-O[1]→O-AD[2]→AD-AG[2]	5778	0.2379	
	7	K-L[2]→L-M[2]→W-M[1]→W-AG[1]	3003	0.8011	
	8	K-L[2]→L-M[1]→W-M[1]→W-AG[1]	3303	0.7766	
	9	K-L[1]→L-M[1]→M-N[1]→N-O[1]→O-AD[1]→AD-AG[1]	6525	0.1889	
	10	K-L[1]→L-M[1]→M-N[2]→N-O[1]→O-AD[1]→AD-AG[1]	5784	0.2379	

the population solutions into several levels according to their dominated solution count. In addition, archive set A is used to store the top solutions found during the search process. In each generation, all non-dominated solutions in the current population are regarded as candidate solutions to update A. If both of the target values of a candidate solution satisfy a non-dominant requirement, the solution is added to A.

E. TERMINATION RULES

In this work, we select the maximum iteration count as the termination rule

Based on the above description, the proposed approach is shown in Fig. 5.

IV. EXPERIMENTAL RESULTS AND ANALYSIS

This section assesses the performance of multimodal transport paths sequence plan problem running experiments. The proposed problem is implemented in MATLAB 2016 A and executed on an Intel(R) Core(TM) i7 CPU (2.53 GHz/4.00-GB RAM) PC with a Windows 10 operating system.

Its parameter values are as follows:

The population size ApopSize = 50, which is equal the number of ants.

The maximum iteration count of DDACO amax = 200.

The amount of Pheromone release in DDACO Q = 1.

The pheromone play factor in DDACO $\rho = 0.2$.

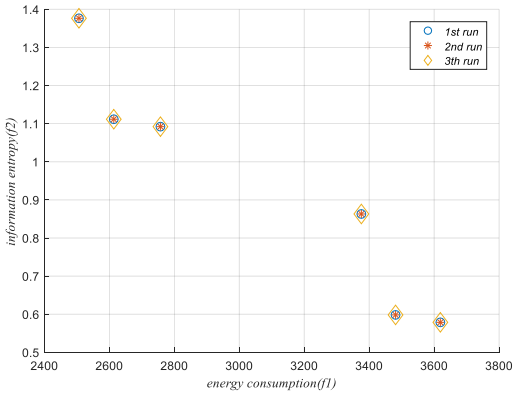

FIGURE 6. Pareto solutions of case study 1 in the objective space.

A. CASE STUDY 1

First, the proposed approach is applied to case 1 in Section II. It has 7 nodes and 14 paths. The parameter values of case 1 are show in Tables 1-8.

The results of the DDACO algorithm are executed for three runs in Table 9. The first column lists the number of runs, and the second one gives the serial number of the Pareto solutions obtained in each run. The third column represents the multimodal transport route solutions obtained in each run. The fourth and fifth columns show f1 and f2 values of the Pareto solutions, respectively. The sixth column gives the computational time for finding the solutions. We can see that the consumed energy and the information entropy in those

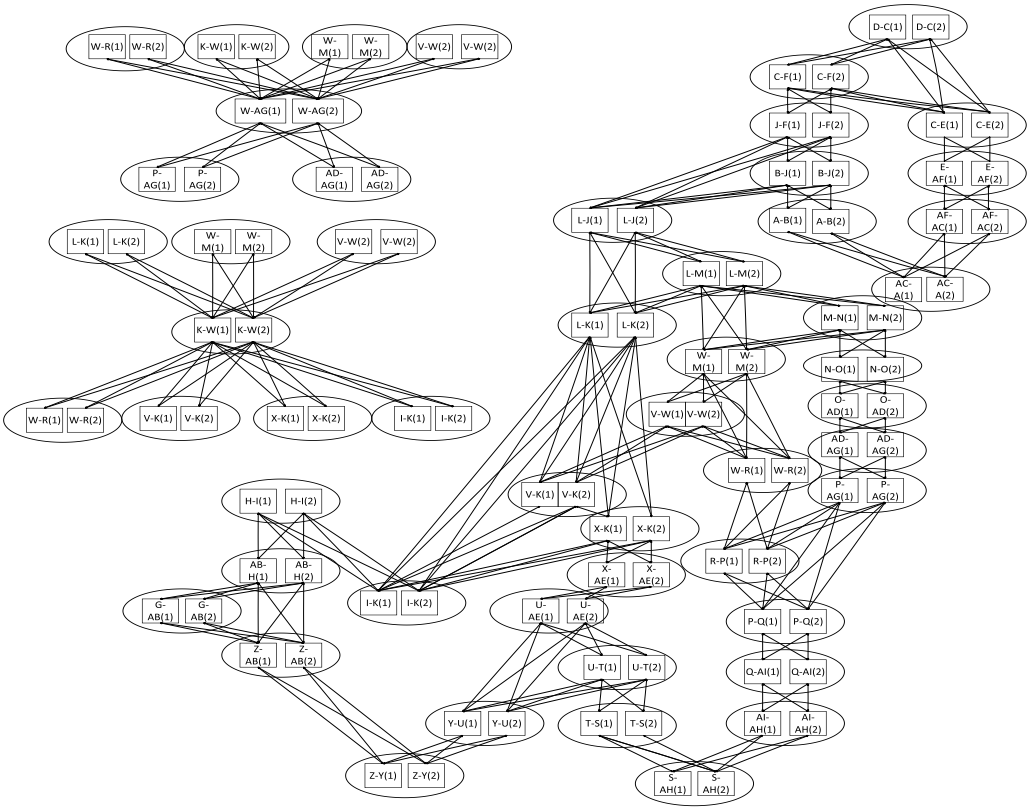

FIGURE 7. The AND/OR graph of the radio set of case study 2.

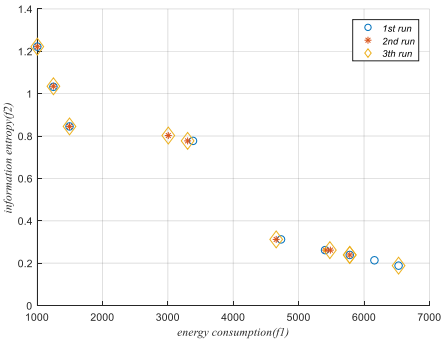

FIGURE 8. Pareto solutions of case study 2 in the objective space.

obtained Pareto solutions fall into [2507.25, 3619.25] and [0.5793, 1.3758], respectively.

The Pareto solutions obtained in the three runs are also shown in Fig. 6. Each run is able to produce the same solutions, which indicates that the algorithm performance is stable. In addition, the average running time for three times is 10.1152 seconds, which indicates the efficiency of the proposed algorithm. Thus, it can effectively solve a multimodal transport optimization problem. We used the spacing metric as the indicator to evaluate the spread performance (SP) of the set. The mean of the results from the three calculations is 17.1490.

B. CASE STUDY 2

To further validate the availability and performance of the DDACO algorithm, we set up another more complex map of multimodal transportation, which simulates the relative positions of 34 provinces in China with 34 notes and 80 paths, shown in Fig. 7. We start at point K and end at point AG. Only road transport, represented by 1, and rail transport, represented by 2, are considered here, and each path has its own transportation capacity constraints. The length of each is in the range [1000, 2000], each path transportation capacity is in the range [1,3], each change in the mode of transportation energy consumption is in the range [1,3], the risk probability in each path is in the range [0.001,0.3], and the weight of each good is in the range [1,3].

From Table 10, for this case, the DDACO algorithm is capable of generating satisfactory results within acceptable time in three runs. Additionally, as the scale of nodes and paths increase, the AOG becomes more complex, such that the computational time to obtain the Pareto solutions is significantly larger. The average running time for three times is 284.3293 seconds. Moreover, Fig. 8 shows the obtained Pareto solutions of this case. We used the Spacing Metric as the indicator to evaluate the spread performance (SP) of the set. The mean of the results from the three calculations is 272.6110. The proposed algorithm is capable of generating highly similar Pareto solutions, and thus it is effective in

solving the proposed multimodal transport route sequences plan problem.

V. CONCLUSIONS

This work addresses a dual-objective multimodal transport path sequence optimization issue based on an AND/OR graph from energy-efficient and risk perspectives for the first time. Its goal is to minimize energy consumption and information entropy in the multimodal transport process. To achieve an AND/OR graph-based heuristic route planning, adjacency and conflict matrices are introduced to describe accessible AND and exclusive OR conflicts among a selected path's relations and constraints. An effective triple-phase generates route method satisfying three constraints is proposed to create feasible path sequences. A dual-objective discrete ant colony is proposed to solve the proposed model. The proposed algorithm can solve the model effectively and efficiently and generate the Pareto solutions of a dual-objective multimodal transport paths sequence optimization problem. The results can be used to guide decision makers in making better decisions when a route is selected in a real multimodal transport process.

Although the efficacy of the proposed model has been verified, certain limitations exist. First, this work does not use actual multimodal transport route data to validate this method to provide the best decision support. Second, with increases in the complexity of the path selected, the calculation time of the information entropy formula increases exponentially. Therefore, to overcome the mentioned limitations, we need to develop more advanced multimodal transport path planning models and methods in the future.

REFERENCES

[1] Z. Wang, L. Zhao, N. Cao, M. Yu, and M. Chen, "The route choice of hazardous material transportation with value-at-risk model using chance measure in uncertain environments," *Adv. Mech. Eng.*, vol. 10, no. 2, pp. 1–13, Feb. 2018.

[2] X. Luan, L. Cheng, Y. Song, and C. Sun, "Performance evaluation and alternative optimization model of light rail transit network projects: A real case perspective," *Can. J. Civil Eng.*, vol. 46, no. 9, pp. 836–846, Sep. 2019.

[3] R. K. Niven, M. Abel, M. Schlegel, and S. H. Waldrip, "Maximum entropy analysis of flow networks: Theoretical foundation and applications," *Entropy*, vol. 21, no. 8, p. 776, Aug. 2019.

[4] S.-I. Amari, R. Karakida, M. Oizumi, and M. Cuturi, "Information geometry for regularized optimal transport and barycenters of patterns," *Neural Comput.*, vol. 31, no. 5, pp. 827–848, May 2019.

[5] M. Wang, X. Lin, and L. Yu, "Comprehensive evaluation of green transportation in Chongqing main urban area based on sustainable development theory," *Syst. Sci. Control Eng.*, vol. 7, no. 1, pp. 369–378, Jan. 2019.

[6] Z. P. Li, C. Xu, L. Chen, and S. Zhou, "Dynamic traffic flow entropy calculation based on vehicle spacing," in *Proc. Int. Conf. Environ. Sci. Mater. Appl.*, Xi'an, China, 2019, pp. 1–7.

[7] B. Chen, Y. Liu, and T. Zhou, "An entropy based solid transportation problem in uncertain environment," *J. Ambient Intell. Hum. Comput.*, vol. 10, no. 1, pp. 357–363, Jan. 2019.

[8] Y. Zhang and P. Shang, "The complexity–entropy causality plane based on multivariate multiscale distribution entropy of traffic time series," *Nonlinear Dyn.*, vol. 95, no. 1, pp. 617–629, Jan. 2019.

[9] C. Zhang, G. Xiao, Y. Liu, and F. Yu, "The relationship between organizational forms and the comprehensive effectiveness for public transport services in China?" *Transp. Res. A, Policy Pract.*, vol. 118, pp. 783–802, Dec. 2018.

[10] L. Dong, A. Rinoshika, and Z. Tang, "Dynamic evaluation on the traffic state of an urban gated community by opening the micro-inter-road network," *Technologies*, vol. 6, no. 3, p. 71, Jul. 2018.

[11] W. Zhou, J. Chen, and B. Ding, "Optimal flow distribution of military supply transportation based on network analysis and entropy measurement," *Entropy*, vol. 20, no. 6, p. 446, Jun. 2018.

[12] B. He, Y. Zhang, Y. Chen, and Z. Gu, "A simple line clustering method for spatial analysis with origin-destination data and its application to bike-sharing movement data," *ISPRS Int. J. Geo-Inf.*, vol. 7, no. 6, p. 203, May 2018.

[13] Y. Chai, M. Zhu, Y. Zhu, Z. Zhang, and Z. Zhang, "On two-dimensional structural information of Beijing transportation networks based on traffic big data," in *Proc. 2nd Int. Conf. Cloud Big Data Comput. (ICCBDC)*, Barcelona, Spain, 2018, pp. 28–32.

[14] W. Peng and Z. Lin, "Research on risk assessment of railway freight station based on nonlinear combination of Ahp-entropy," in *Proc. 15th Int. Conf. Service Syst. Service Manage. (ICSSSM)*, Hangzhou, China, Jul. 2018, pp. 1–6.

[15] M. Noussan and S. Tagliapietra, "The effect of digitalization in the energy consumption of passenger transport: An analysis of future scenarios for Europe," *J. Cleaner Prod.*, vol. 258, Jun. 2020, Art. no. 120926.

[16] A. Wang, R. Tu, Y. Gai, L. G. Pereira, J. Vaughan, I. D. Posen, E. J. Miller, and M. Hatzopoulou, "Capturing uncertainty in emission estimates related to vehicle electrification and implications for metropolitan greenhouse gas emission inventories," *Appl. Energy*, vol. 265, May 2020, Art. no. 114798.

[17] Y. V. Fan, J. J. Klemeš, T. G. Walmsley, and S. Perry, "Minimising energy consumption and environmental burden of freight transport using a novel graphical decision-making tool," *Renew. Sustain. Energy Rev.*, vol. 114, Oct. 2019, Art. no. 109335.

[18] Z. A. Needell and J. E. Trancik, "Efficiently simulating personal vehicle energy consumption in mesoscopic transport models," *Transp. Res. Rec., J. Transp. Res. Board*, vol. 2672, no. 25, pp. 163–173, Dec. 2018.

[19] F. Rehermann and M. Pablo-Romero, "Economic growth and transport energy consumption in the Latin American and Caribbean countries," *Energy Policy*, vol. 122, pp. 518–527, Nov. 2018.

[20] Q. Zhang, X. Ou, and X. Zhang, "Future penetration and impacts of electric vehicles on transport energy consumption and CO_2 emissions in different Chinese tiered cities," *Sci. China Technol. Sci.*, vol. 61, no. 10, pp. 1483–1491, Oct. 2018.

[21] M. G. Mouna and S. Bouamama, "Multi-layer distributed constraint satisfaction for multi-criteria optimization problem: Multimodal transportation network planning problem," *Int. J. Appl. Metaheuristic Comput.*, vol. 11, no. 2, pp. 134–155, 2020.

[22] A.-B. Laurent, S. Vallerand, Y. van der Meer, and S. D'Amours, "CarbonRoadMap: A multicriteria decision tool for multimodal transportation," *Int. J. Sustain. Transp.*, vol. 14, no. 3, pp. 205–214, Jan. 2020.

[23] H. Li and L. Su, "Multimodal transport path optimization model and algorithm considering carbon emission multitask," *J. Supercomput.*, pp. 1–19, Feb. 2020.

[24] Y. Sun, "Green and reliable freight routing problem in the road-rail intermodal transportation network with uncertain parameters: A fuzzy goal programming approach," *J. Adv. Transp.*, vol. 2020, pp. 1–21, Feb. 2020.

[25] X. Fang, Z. Ji, Z. Chen, W. Chen, C. Cao, and J. Gan, "Synergy degree evaluation of container multimodal transport system," *Sustainability*, vol. 12, no. 4, p. 1487, Feb. 2020.

[26] D. Chen, Y. Zhang, L. Gao, and R. G. Thompson, "Optimizing multimodal transportation routes considering container use," *Sustainability*, vol. 11, no. 19, p. 5320, Sep. 2019.

[27] Y. Zhao, P. A. Ioannou, and M. M. Dessouky, "Dynamic multimodal freight routing using a co-simulation optimization approach," *IEEE Trans. Intell. Transp. Syst.*, vol. 20, no. 7, pp. 2657–2667, Jul. 2019.

[28] G. Tian, N. Hao, M. Zhou, W. Pedrycz, C. Zhang, F. Ma, and Z. Li, "Fuzzy grey Choquet integral for evaluation of multicriteria decision making problems with interactive and qualitative indices," *IEEE Trans. Syst., Man, Cybern., Syst.*, early access, Apr. 12, 2019, doi: doi:.10.1109/TSMC.2019.2906635.

[29] G. Tian, M. Zhou, and P. Li, "Disassembly sequence planning considering fuzzy component quality and varying operational cost," *IEEE Trans. Autom. Sci. Eng.*, vol. 15, no. 2, pp. 748–760, Apr. 2018.

[30] G. Tian, Y. Ren, Y. Feng, M. Zhou, H. Zhang, and J. Tan, "Modeling and planning for dual-objective selective disassembly using and or graph and discrete artificial bee colony," *IEEE Trans. Ind. Informat.*, vol. 15, no. 4, pp. 2456–2468, Apr. 2019.

[31] G. Tian, H. Zhang, Y. Feng, H. Jia, C. Zhang, Z. Jiang, Z. Li, and P. Li, "Operation patterns analysis of automotive components remanufacturing industry development in China," *J. Cleaner Prod.*, vol. 164, pp. 1363–1375, Oct. 2017.
[32] W. Wang, G. Tian, M. Chen, F. Tao, C. Zhang, A. AI-Ahmari, Z. Li, and Z. Jiang, "Dual-objective program and improved artificial bee colony for the optimization of energy-conscious milling parameters subject to multiple constraints," *J. Cleaner Prod.*, vol. 245, Feb. 2020, Art. no. 118714, doi: 10.1016/j.jclepro.2019.118714.
[33] D. I. Arkhipov, D. Wu, T. Wu, and A. C. Regan, "A parallel genetic algorithm framework for transportation planning and logistics management," *IEEE Access*, vol. 8, pp. 106506–106515, 2020.
[34] J. Li, Y. Xia, B. Li, and Z. Zeng, "A pseudo-dynamic search ant colony optimization algorithm with improved negative feedback mechanism," *Cognit. Syst. Res.*, vol. 62, pp. 1–9, Aug. 2020.
[35] M. Starzec, G. Starzec, A. Byrski, W. Turek, and K. Pi tak, "Desynchronization in distributed ant colony optimization in HPC environment," *Future Gener. Comput. Syst.*, vol. 109, pp. 125–133, Aug. 2020.
[36] N. Yi, J. Xu, L. Yan, and L. Huang, "Task optimization and scheduling of distributed cyber–physical system based on improved ant colony algorithm," *Future Gener. Comput. Syst.*, vol. 109, pp. 134–148, Aug. 2020.
[37] V. Arora, M. Singh, and R. Bhatia, "Orientation-based ant colony algorithm for synthesizing the test scenarios in UML activity diagram," *Inf. Softw. Technol.*, vol. 123, Jul. 2020, Art. no. 106292.
[38] S. Ebadinezhad, "DEACO: Adopting dynamic evaporation strategy to enhance ACO algorithm for the traveling salesman problem," *Eng. Appl. Artif. Intell.*, vol. 92, Jun. 2020, Art. no. 103649.
[39] H. Zhang, H. Nguyen, X.-N. Bui, T. Nguyen-Thoi, T.-T. Bui, N. Nguyen, D.-A. Vu, V. Mahesh, and H. Moayedi, "Developing a novel artificial intelligence model to estimate the capital cost of mining projects using deep neural network-based ant colony optimization algorithm," *Resour. Policy*, vol. 66, Jun. 2020, Art. no. 101604.
[40] Y. Wang, L. Wang, G. Chen, Z. Cai, Y. Zhou, and L. Xing, "An improved ant colony optimization algorithm to the periodic vehicle routing problem with time window and service choice," *Swarm Evol. Comput.*, vol. 55, Jun. 2020, Art. no. 100675.
[41] Z. A. Çil, S. Mete, and F. Serin, "Robotic disassembly line balancing problem: A mathematical model and ant colony optimization approach," *Appl. Math. Model.*, vol. 86, pp. 335–348, Oct. 2020.
[42] H. Zhang, Z.-H. Jia, and K. Li, "Ant colony optimization algorithm for total weighted completion time minimization on non-identical batch machines," *Comput. Oper. Res.*, vol. 117, May 2020, Art. no. 104889.
[43] S. S. Singh, K. Singh, A. Kumar, and B. Biswas, "ACO-IM: Maximizing influence in social networks using ant colony optimization," *Soft Comput.*, vol. 24, no. 13, pp. 10181–10203, Jul. 2020.
[44] S. S. Singh, K. Singh, A. Kumar, and B. Biswas, "ACO-IM: Maximizing influence in social networks using ant colony optimization," *Soft Comput.*, vol. 24, no. 13, pp. 10181–10203, Jul. 2020.
[45] D. L. Pereira, J. C. Alves, and M. C. D. O. Moreira, "A multiperiod workforce scheduling and routing problem with dependent tasks," *Comput. Oper. Res.*, vol. 118, Jun. 2020, Art. no. 104930.
[46] Q. Li, X. Wang, and X. Zhang, "A scheduling method based on NSGA2 for steelmaking and continuous casting production process," *IFAC-PapersOnLine*, vol. 51, no. 18, pp. 174–179, 2018.
[47] W. Jiasen and G. Longqin, "Left-right crowding distance (LRCD) calculation method in NSGA2 to preserve diversity distribution," in *Proc. 3rd Int. Conf. Comput. Sci. Inf. Technol.*, Chengdu, China, Jul. 2010, pp. 211–215.
[48] C.-T. Yeh, "An improved NSGA2 to solve a bi-objective optimization problem of multi-state electronic transaction network," *Rel. Eng. Syst. Saf.*, vol. 191, Nov. 2019, Art. no. 106578.
[49] C. Khammassi and S. Krichen, "A NSGA2-LR wrapper approach for feature selection in network intrusion detection," *Comput. Netw.*, vol. 172, May 2020, Art. no. 107183.
[50] U. Singh and S. N. Singh, "Optimal feature selection via NSGA-II for power quality disturbances classification," *IEEE Trans. Ind. Informat.*, vol. 14, no. 7, pp. 2994–3002, Jul. 2018.

ZHANZHONG WANG received the B.S. degree in transportation planning and management from the Jilin University of Technology, Changchun, China, in 1986, and the M.S. degree in transportation planning and management and the Ph.D. degree in carrying tools applied engineering from Jilin University, Changchun, in 1989 and 2007, respectively. He worked at Jilin Province Transportation Administration Bureau, from 1989 to 1997, and at Jilin Ji Transport Group Company Ltd., from 1997 to 2002. He is currently a Professor with Jilin University, devotes himself to transport resources optimization technology, mainly in the direction of production logistics operation, transportation economy and national economy evaluation, integrated transportation, and traffic big data analysis.

MINGHANG ZHANG is currently pursuing the master's degree with the School of Transportation, Jilin University, Changchun, China. His research interests include multimodal transport, data mining, and machine learning.

RUIJUAN CHU is currently pursuing the Ph.D. degree with the School of Transportation, Jilin University, Changchun, China. Her research interests include integrated freight transportation corridors, data mining, machine learning, and traffic big data analysis.

LIYING ZHAO received the Ph.D. degree in transportation planning and management from the Transportation College, Jilin University, in 2018. She is currently a young Teacher with the Department of Management Science and Engineering, Xi'an University of Technology. Her current research includes logistics system and uncertain optimization theory.